Optical Engineering

SPIEDigitalLibrary.org/oe

Improving the uniformity of luminous system in radial imaging capsule endoscope system

Mang Ou-Yang
Wei-De Jeng

Improving the uniformity of luminous system in radial imaging capsule endoscope system

Mang Ou-Yang
National Chiao-Tung University
Department of Electrical and Computer Engineering
University Road 1001
Hsinchu 30010, Taiwan

Wei-De Jeng
National Chiao-Tung University
Department of Electrical and Control Engineering
University Road 1001
Hsinchu 30010, Taiwan
E-mail: jwd.ece99g@nctu.edu.tw

Abstract. This study concerns the illumination system in a radial imaging capsule endoscope (RICE). Uniformly illuminating the object is difficult because the intensity of the light from the light emitting diodes (LEDs) varies with angular displacement. When light is emitted from the surface of the LED, it first encounters the cone mirror, from which it is reflected, before directly passing through the lenses and complementary metal oxide semiconductor (CMOS) sensor. The light that is strongly reflected from the transparent view window (TVW) propagates again to the cone mirror, to be reflected and to pass through the lenses and CMOS sensor. The above two phenomena cause overblooming on the image plane. Overblooming causes nonuniform illumination on the image plane and consequently reduced image quality. In this work, optical design software was utilized to construct a photometric model for the optimal design of the LED illumination system. Based on the original RICE model, this paper proposes an optimal design to improve the uniformity of the illumination. The illumination uniformity in the RICE is increased from its original value of 0.128 to 0.69, greatly improving light uniformity. [DOI: 10.1117/1.OE.52.2.023003]

Subject terms: radial imaging capsule endoscope; illumination system; light uniformity; optimal design.

Paper 121256P received Aug. 31, 2012; revised manuscript received Jan. 14, 2013; accepted for publication Jan. 16, 2013; published online Feb. 19, 2013.

1 Introduction

Human beings have suffered from digestive system diseases for a long time. The capsule endoscope system is utilized to identify pathological changes in the alimentary canal of the small intestine. The optical structure of a capsule endoscope comprises a light source, optical lenses, and a CMOS sensor. Doctors insert the device into the body of a patient to capture images of the intestine,[1,2] which they analyze based on experience. Unfortunately, the front imaging capsule endoscope (FICE) has some disadvantages.[3,4] For example, wrinkles in the intestine produce dead pixels, making difficult the reconstruction of the images and requiring a long depth of view.[3,4] Accordingly, the radial imaging capsule endoscope (RICE) was developed.[3]

Although the RICE system can solve the aforementioned problems, it still requires important improvements, one of which is in the area of lighting. The illumination of RICE is very different from that of FICE. Figure 1 shows the illumination utilized in the RICE and the FICE. The FICE uses an optical elliptical dome to solve the problem of stray light. In this method, an LED is placed on the focal plane of the elliptical dome, and stray light is reflected to another LED, based on Fermat's principle.[5] In the RICE, this method cannot be used to solve the stray light problem, so the uniformity of light in the FICE is better than that in the RICE.[6] In this work, the Advanced Systems Analysis Program (ASAP) is used to simulate the illumination and optimize that of a radial imaging capsule endoscope. The distribution of light is not uniform on the object plane when the RICE moves in the intestine, so image quality is detrimentally affected. However, the strongly reflected light from the cone mirror or the capsule shell may enter the CMOS, preventing the doctor from accurately assessing the disease. Therefore, this paper proposes an optimal design of illumination system. The uniformity of light in a capsule endoscope can be improved by changing the position of the LED or the direction of lighting, coating the view window, or cutting some parts out of the cone mirror. These improvements were made in a prototype illumination system for RICE, and the light uniformity is increased higher than a FICE system.

2 Analysis of Illumination in RICE

Several factors can affect an illumination system. In the RICE system, stray light causes severe illumination problems because the system is tiny. To solve this problem, this study analyzes the source of stray light and quantifies the uniformity of light in a RICE system.

2.1 *Stray Light in RICE*

Stray light in RICE can be divided into two types—direct and indirect. First, direct stray light, shown in Fig. 2(a), consists of several rays emitted from the LED which are reflected at the cone mirror and pass through the lens, before being received by the detector. These rays are received by the detector without any image information. The other type of stray light, shown in Fig. 2(b), comprises rays that are emitted from the LED, reflected on the cone mirror, and then propagate to the transparent view window (TVW), where they are reflected returning to the cone mirror to be reflected again, before passing through the lens to be received by the detector without any image information. Since the TVW is

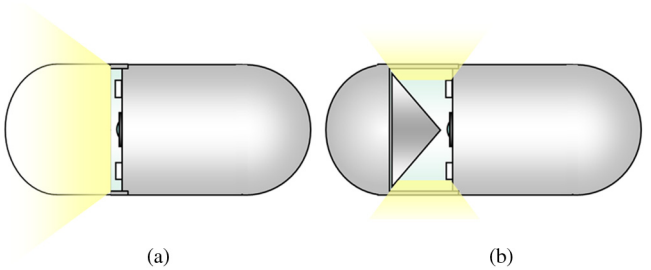

Fig. 1 Illumination methods between (a) FICE and (b) RICE.

responsible for this phenomenon, the stray light is regarded as indirect. Therefore, two elements affect the uniformity of light in a RICE system: the cone mirror and the TVW. In the following section, ASAP is utilized to simulate and optimize the uniformity of light in RICE.

2.2 *Definition of Uniformity of Light in RICE*

As mentioned in Sec. 2.1, the low uniformity of light in a RICE system is caused by the serious stray light problems. Most attempts to quantify the uniformity of illumination use a formula that equates light uniformity to the ratio of mean irradiance, E_{avg}, to maximum irradiance, E_{max}, as in Eq. (1).

$$\text{Uniformity} = \frac{E_{avg}}{E_{max}}. \tag{1}$$

According to Eq. (1), a higher E_{max} corresponds to lower uniformity. When the stray light is distributed widely or has high intensity, the stray light dominates E_{max}. Therefore, stray light should be considered in the computation of the uniformity of light in the RICE, and the above formula becomes inappropriate. For example, assume that the values of irradiance of all pixels on the detector are almost equal; the uniformity is almost one; in contrast, if a pixel has a high irradiance (stray light) that exceeds E_{avg}, the uniformity will be greatly reduced, because the pixel is a singular point. To accommodate this situation, the definition of uniformity should be changed to that in Eq. (2). The term σ is standard deviation, and the denominator $E_{avg} + 2\sigma$ is standard in statistics. The intensity of light on the image plane is normally distributed, because it is higher at the center than the outers, like a Gaussian distribution. Hence, the empirical rule is taken into consideration.[7–9]

$$\text{Uniformity} = \frac{E_{avg}}{E_{avg} + 2\sigma}. \tag{2}$$

3 Modeling Illumination System of RICE with Experimental Verification

For modeling purposes, a RICE system can be divided into two parts—the imaging system and the nonimaging system. The elements of the imaging system are the lenses and cone mirror, and those of the nonimaging system are the LED and the printed circuit board (PCB). The RICE illumination system, described elsewhere, is obtained by combining the two parts.[6] The specifications of the lenses and cone mirror can be found elsewhere.[3] In this simulation, the TVW is made of a transparent material, and an annular object of radius 6.4 mm and length 5.825 mm is used to mimic the intestine. The resolution of the detector is 512×512, and the pixel size is 5.6 μm. The sizes of the PCB and LED are determined by layout specification consistent with a layout that can be found elsewhere.[6] In this work, the most important component is the light source. The illuminator in the RICE is a Nichia LED, with part number NESWC04T as described in Ref. 10. The number of rays that are emitted from each LED is set to 1,000,000, and the total flux is 100 mW. After the properties of all optical elements have been defined, the original model of RICE is built in ASAP. Figure 3 shows the three-dimensional layout of the RICE system. In this work, the field of view is separated into five parts to analyze the results more effectively.

Figure 4(a) shows the original results of the simulation of the original design. Clearly, the third field has six light spots, such that the space between them is 60 deg. To clarify this phenomenon, another case is considered, in which the TVW is removed. For comparison, Fig. 4(b) shows the results of the simulation without TVW.

As Fig. 4(b) shows, with the TVW removed, the six light spots disappear. However, stray light remains in the second field. According to these results, the TVW changes the lighting. The cone mirror is responsible for most of the stray light in the second field: the mirror reflects the light that is emitted from the LED; the reflected light passes through the lens and

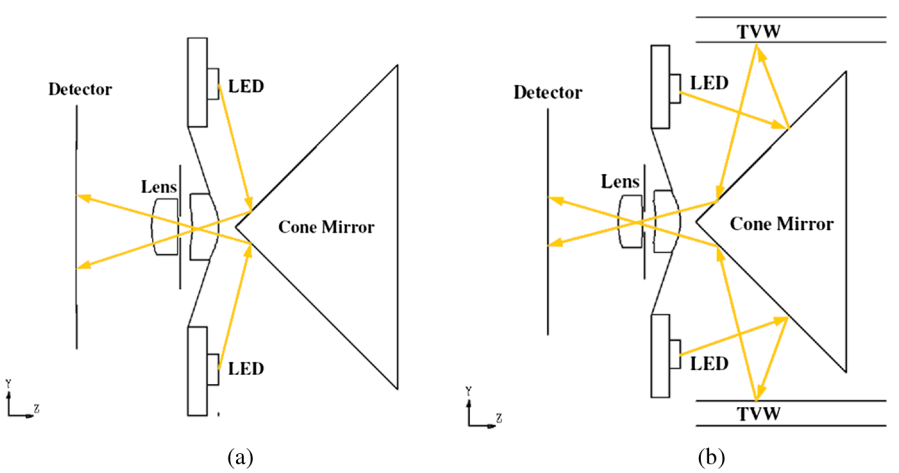

Fig. 2 (a) Direct and (b) indirect stray light issues in RICE.

stops on the detector. In the other case, the TVW produces the light spots. Since the TVW is not a totally reflecting optical element, it will reflect some of the light, which ultimately propagates to the detector again. Both causes of stray light must be mitigated to increase the uniformity of illumination.

To investigate the RICE model that was constructed using ASAP, an experiment was conducted to identify the stray light distribution in a real case. The object is divided into five fields and is rolled into an object tube to enable the radial direction to be easily scanned in the RICE system, as shown in Fig. 5.[3]

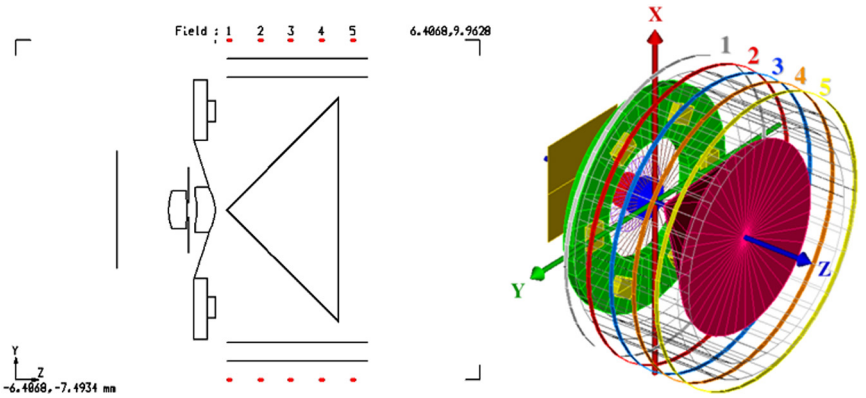

(a) (b)

Fig. 3 Model of the RICE system with two-dimensional (a) and three-dimensional (b) layouts.

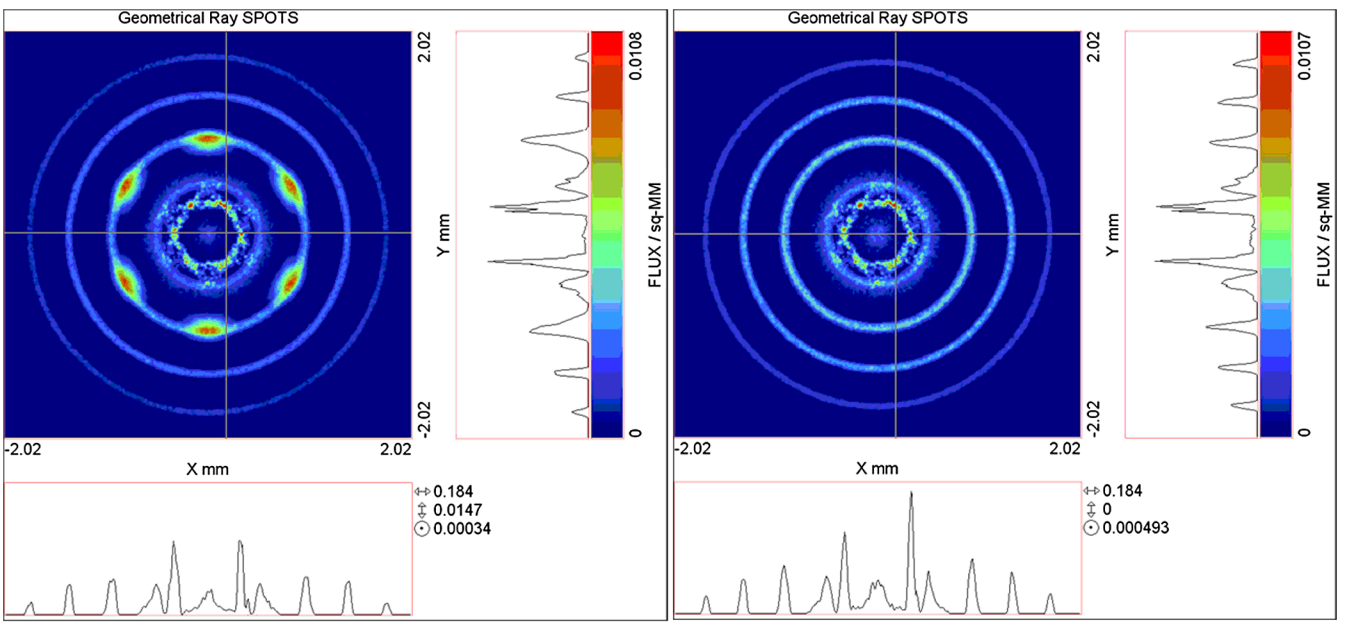

(a) (b)

Fig. 4 Simulation results of power distribution (a) with TVW and (b) without TVW.

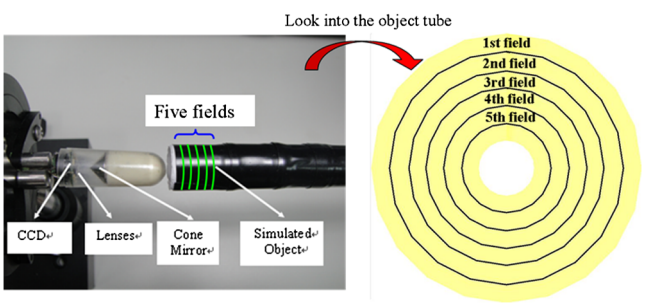

(a) (b)

Fig. 5 Experimental setup for verifying the stray light issue (a), and the inner pattern of the simulated object (b).

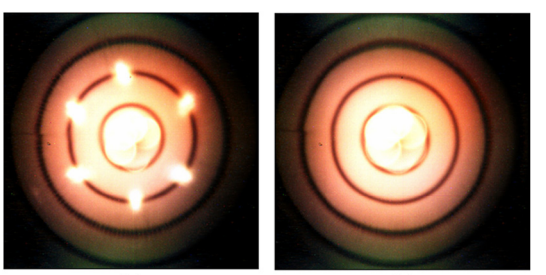

(a) (b)

Fig. 6 Light distribution on the imaging plane (a) with TVW and (b) without TVW. The most significant difference is the six light spots at the image center, which is similar to the simulation results.

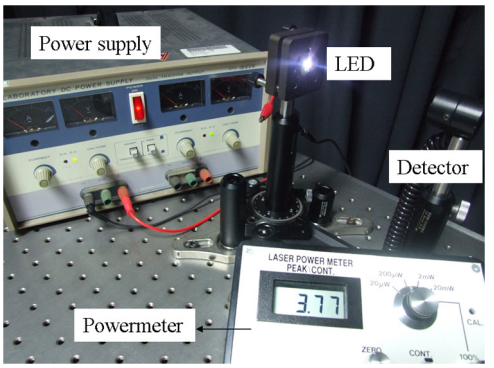

Fig. 7 The experimental environment includes a two-dimensional rotating platform, a power supply, and a power meter.

Figure 6 shows the experimental results. The overblooming at the center of the image makes the first field too dark to be recognized. The similarity between the two images arises from the distribution of the stray light in the second field. The light spot distribution of the two images is different. When the TVW is utilized, light spots appear in the third field; without TVW, they do not. Although the simulation and experimental results are mutually consistent, the diffraction effect should be discussed in more detail.

According to scalar diffraction theory, the propagation of light can be divided into near-field and far-field. In recent years, C. C. Sun considered the importance of the midfield region, which is between the near-field and far-field regions; in this region, the propagation of light varies with distance, normally within 1 cm to 1 m.[11,12] This case applies in RICE because the distance from the LED to the image plane is only a few centimeters. Experiments were carried out to verify the accuracy of the simulation. To quantify the similarity between the simulated and experimental results, the normalized cross correlation (NCC) formula, as in Eq. (3), is used, where A_{xy} and B_{xy} are the intensity of simulation and experimental values, $\bar{A}$ and $\bar{B}$ are the mean values of A and B. Figure 7 shows the experimental environment. The LED is fixed on a rotating platform to measure its light intensity at various angles; a power meter is located at different distances to measure light intensity, and a power supply provides DC current to the LED.

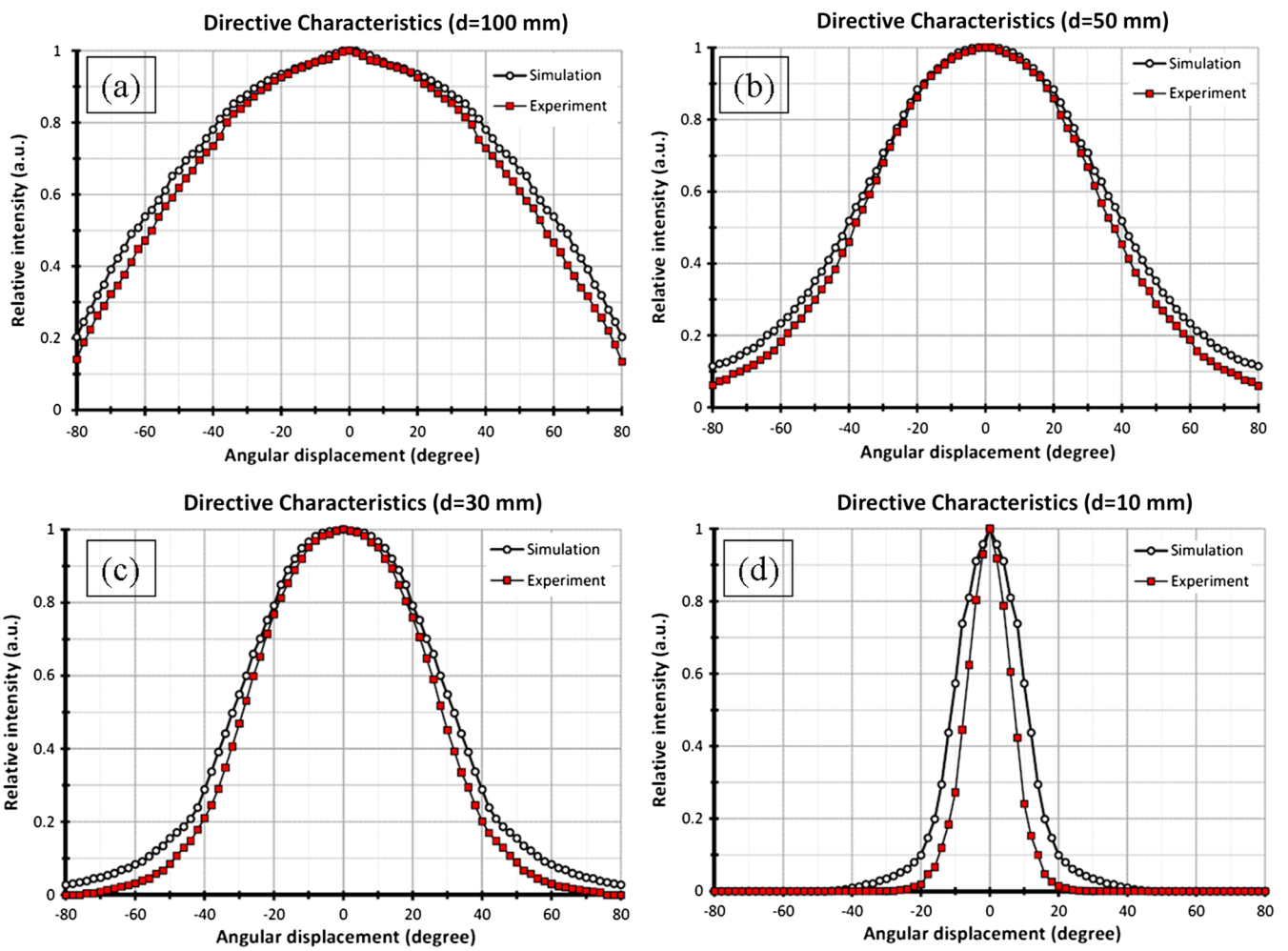

Fig. 8 The directive characteristics of LEDs at different distances, (a) 100 mm, (b) 50 mm, (c) 30 mm, and (d) 10 mm. The directive characteristics vary at different distances in the midfield region.

Table 1 The NCC values between simulation and experimental results.

Data	Experiment and simulation (horizontal axis)			
Index	$d = 100$ mm	$d = 50$ mm	$d = 30$ mm	$d = 10$ mm
NCC	99.87%	99.89%	99.83%	98.13%

$$\mathrm{NCC} = \frac{\sum_x \sum_y (A_{xy} - \bar{A})(B_{xy} - \bar{B})}{\sqrt{\sum_x \sum_y (A_{xy} - \bar{A})^2 \sum_x \sum_y (B_{xy} - \bar{B})^2}}. \quad (3)$$

Figure 8 shows the patterns of light at various distances. The light patterns clearly vary with distance in the midfield region. However, the simulated and experimental light patterns are very similar, and the NCC values are shown in Table 1. At all distances, the NCC values exceed 98%, indicating that the optical model that is constructed in ASAP is highly accurate. After the RICE model is constructed, the initial design and optimization can be carried out.

4 Design of the Illumination System in RICE System

4.1 *Initial Design of Illumination System in RICE*

The RICE system suffers from stray light because it includes a cone mirror and a TVW. Such stray light can be categorized as direct or indirect. This section focuses on reducing direct stray light by changing the optical components in the RICE. To determine which factor is responsible for direct stray light, a simulation is carried out without a TVW. Figure 9 shows the results of the simulation. Figure 9(a) shows some light spots and scattering at the center of the image. These phenomena are generated by the cone mirror or the object. To determine which component dominates, the absorbance of the object is set to 100%. The simulation results in Fig. 9(b) reveal light scattering, indicating that the direct stray light is caused by the cone mirror, because both with and without the setting of the absorptance of the object to 100%, light spots are obtained. Therefore, the critical task in solving the problem of direct stray light must involve the cone mirror.

The simulation results in Fig. 9 include light spots that are concentrated at the center of the image. A comparison with the other problem in RICE, aberration, shows that the cone mirror causes serious astigmatism in the first to third fields.[3,13,14] These two problems overlap in the same region, greatly reducing the image quality. The problem of lighting and imaging can easily be solved by cutting out the part of the cone mirror that corresponds to the imaging plane in the first to third fields. Figure 10 shows the geometry of a RICE. The image length $\overline{IJ}$ corresponds to the first to third fields, and these three fields of the image have poor image quality which is undesired. According to Gaussian conjugate imaging, this image range corresponds to the object $\overline{BH}$ and $\overline{DE}$.[5] The term r' can be computed to determine how to cut the cone mirror by the similar triangles ΔOBH and ΔODE as shown in Eq. (4). Since the length of o' is $\overline{DF}/2$ from the first to the third fields, r' can be determined to be 0.23 mm. Therefore, the case with the cut cone mirror can be simulated using various values of r' from 0 to 0.23 mm.

$$\frac{o'}{r'} = \frac{\overline{DE}}{\overline{BH}} = \frac{\overline{OD}}{\overline{OB}}, \qquad \overline{BH} = \overline{AB}. \quad (4)$$

Figure 11 shows the simulation results obtained by cutting the cone mirror. Stray light is obtained on the center of the image when r' is less than 0.11 mm. In contrast, when r' exceeds 0.13 mm, the stray light problem is eliminated and the uniformity of light increases to approximately

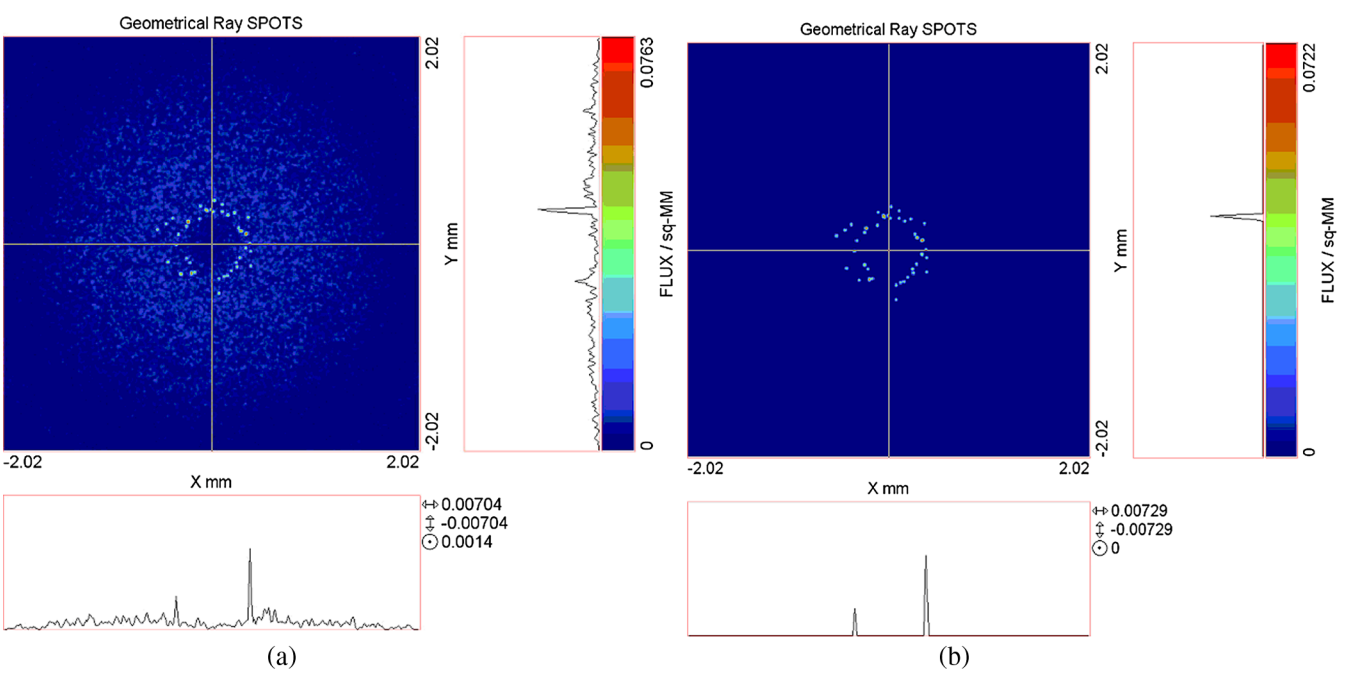

Fig. 9 Power distribution on the imaging detector when the absorptance of the object is set to (a) 50% and (b) 100%.

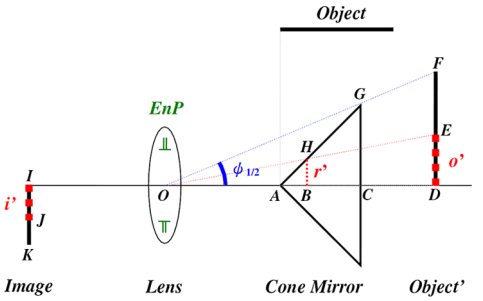

Fig. 10 The geometric relation between image and object. From the similar triangles, the undesired cone mirror part can be computed.

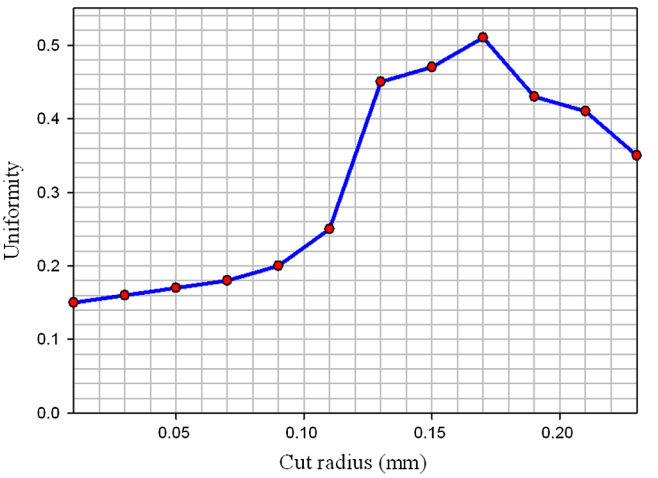

Fig. 12 Uniformity of light by the cut radius r'. The best light uniformity increases to 0.5 by cutting the cone mirror at 0.17 mm.

0.5 when r' equals 0.17 mm, as shown in Fig. 12. Although this behavior may be understood to compromise the imaging region, this issue can be totally resolved by image processing in a manner that can construct all of the image information.[15]

4.2 *Optimizing Illumination System by Reducing Indirect Stray Light*

The direct stray light is generated by the cone mirror, and this problem of stray light can be solved by cutting out some parts of the cone mirror. However, when the simulation includes the TVW, the initial settings of the geometric parameter are as shown in Fig. 13. The six LEDs are all at radii of 3.7 mm; the PCB is at −0.8 mm on the Z axis position; the tilt angle of each LED is 0 deg, and the radius of the cut of the cone mirror is 0.17 mm. Figure 14 shows the results of the simulation of the initial design. Light spots clearly appear when the TVW is included in the simulation, because of the scattering of light on the surface of the TVW. Various methods were utilized to reduce the indirect stray light. These include axially displacing the PCB, changing the radial direction of the LED, tilting the LED, and even coating the TVW.

Figure 15 shows how the various LED positions were changed. The LED is attached to the PCB. Simulations were carried out for various Z_{PCB} positions. When the Z_{PCB} moves in the positive Z direction, the LED moves closer to the cone mirror. R_{LED} denotes the distance between the central point of the LED and the optical axis. Tilting the LED changes the direction of the lighting. When the LED surface faces the object plane, the LED is tilted clockwise; when the LED surface faces the opposite side, the LED is

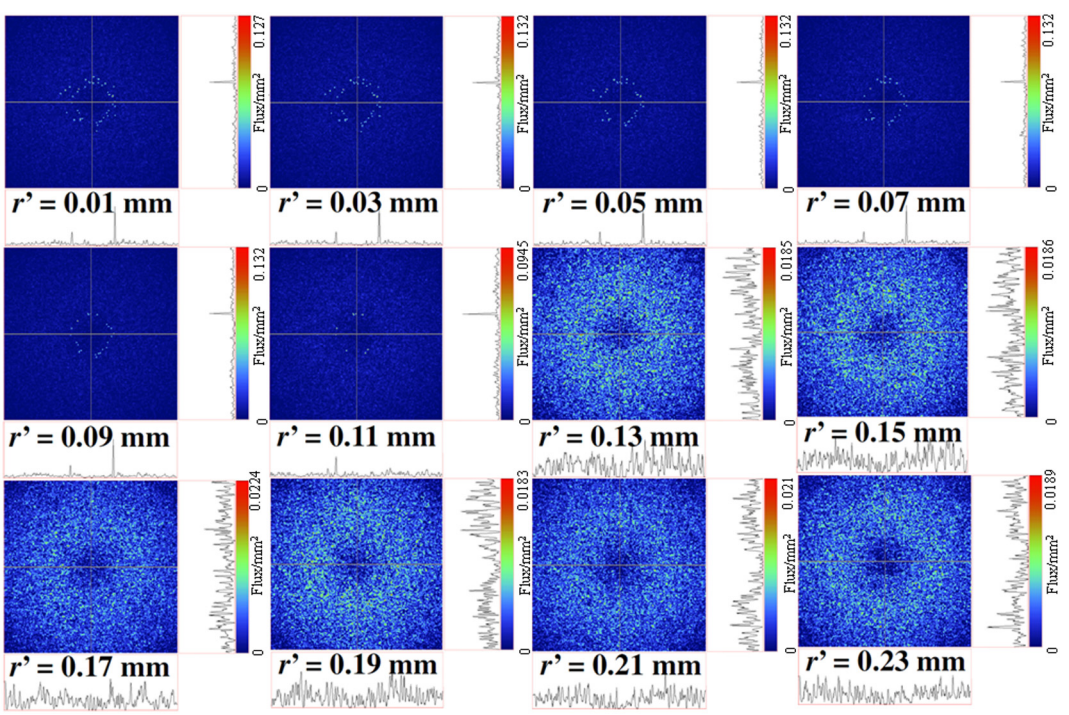

Fig. 11 Simulation results after cutting some parts of the cone mirror. When r' increases, the light spots at the image center disappear and the light uniformity increases.

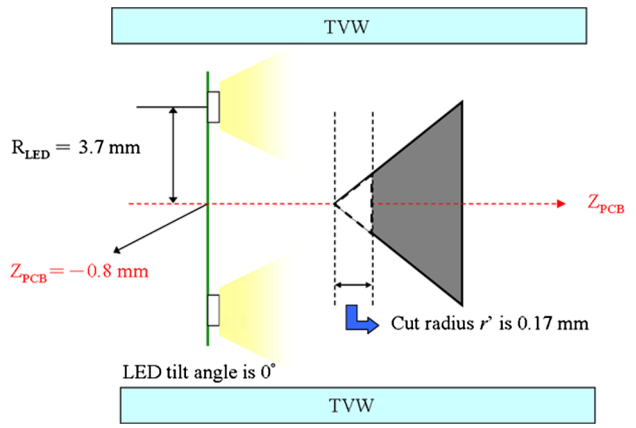

Fig. 13 Initial design parameters of the illumination system in RICE.

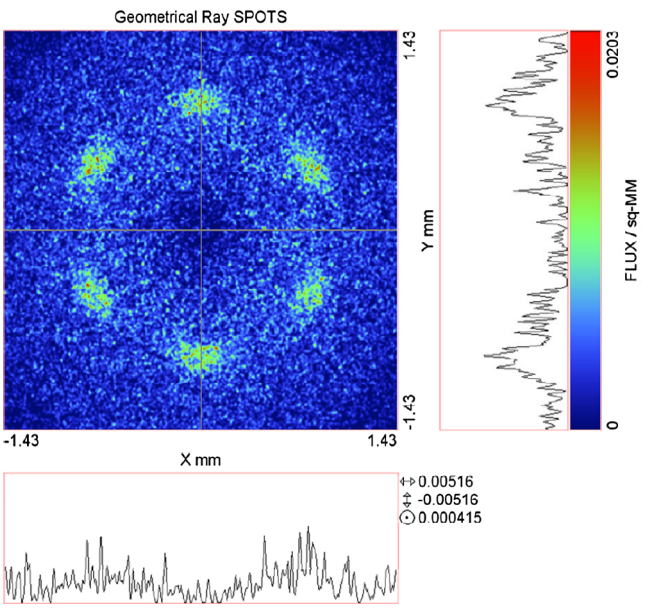

Fig. 14 Simulation result of initial design with TVW.

tilted counterclockwise. The steps in the simulation are as follows:

1. Determine the uniformity of light as the Z_{PCB} position is varied in the simulation.
2. Find the best Z_{PCB} position, which is associated with the maximal light uniformity.
3. Fix the best Z_{PCB} position and then change optimal methods and begin the simulation.
4. Repeat steps 2 and 3 to find the best position for R_{LED} and the angle of tilt.
5. Complete the optimization process.

Figure 16 shows the simulation results that were obtained using three methods. Moving the PCB position does not significantly affect the uniformity because the rays propagate all within 0.3 mm (−1.00 to −0.70 mm) and do not vary the light pattern too much. The other two methods affect the uniformity more significantly, and the uniformity decreases as R_{LED} increases. This result is explained by the fact that a

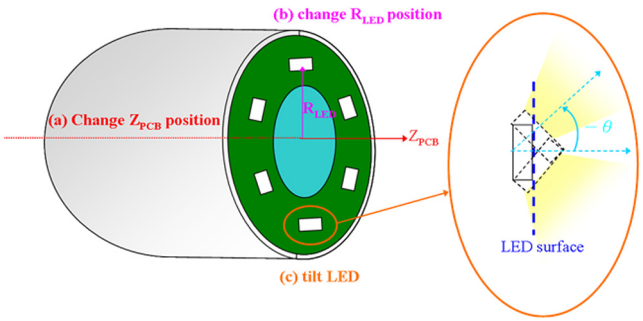

Fig. 15 The optimization design methods are (a) move the PCB on the Z axis, (b) move the LED on the radial direction, and (c) tilt the LED. The LED surface faces the object plane when tilted clockwise and faces the other side when tilted counterclockwise.

small R_{LED} means that the six LEDs are closer to each other and that these rays can be treated as propagating from a single light source, such that the lighting space becomes uniform. In the method of tilting the LED to change the direction of the lighting, when the direction of the lighting faces the object and the tilt angle is −5 deg, the uniformity is maximal. In summary, the best conditions for reducing the indirect stray light are a Z_{PCB} position of −0.7 mm, an R_{LED} position of 3 mm, and a tilt angle of −5 deg. Figure 17 plots the power distribution on the image plane corresponding to three simulation results, and the uniformity is about 0.52, higher than the value of 0.45 achieved with the old design without cutting the cone mirror.[6]

Although the optimal design has a better uniformity than the previous design, six light spots remain in the image plane since the rays are scattered from the TVW. Therefore, the TVW is critical in this system. In the following, an antireflection coating (ARC) was used to improve scattering. Figure 18 shows the simulation results. The antireflection coating on the TVW makes the six light spots difficult to identify. Coating the TVW with a single layer yields a reflectance of 0.75%, which is lower than that, 5.3%, without a coating. To further reduce the reflectance of the TVW, the TVW can be coated on both the inside and the outside by a multilayer coating process. Figure 19 and Table 2 show the results of coating on the TVW. The reflectance of the TVW is almost zero when a multilayer coating is applied to both sides, yielding a uniformity of 0.69, which is 132% higher (from 0.52 to 0.69) than that without a coating.

4.3 *Modeling the Illumination System of FICE to Compare with RICE*

In order to compare the illumination uniformity between FICE and RICE, this section discusses how to build the FICE model which is very similar to RICE. The differences between these two systems are the cone mirror and view window, since the FICE system uses doublet lenses to capture the front side images. As mentioned in the Introduction, the FICE can use an elliptical dome to solve the stray light problem, so the six LEDs are placed on the focal plane of the elliptical dome. The FICE model is shown in Fig. 20. The six LEDs are the same type as in the RICE, and the distance between each LED and the optical axis is also the same. The material of the optical dome is PU (DOW PLASTIC) ISOPLAST* 2530, which matches the organ tissue adaptability of human body.

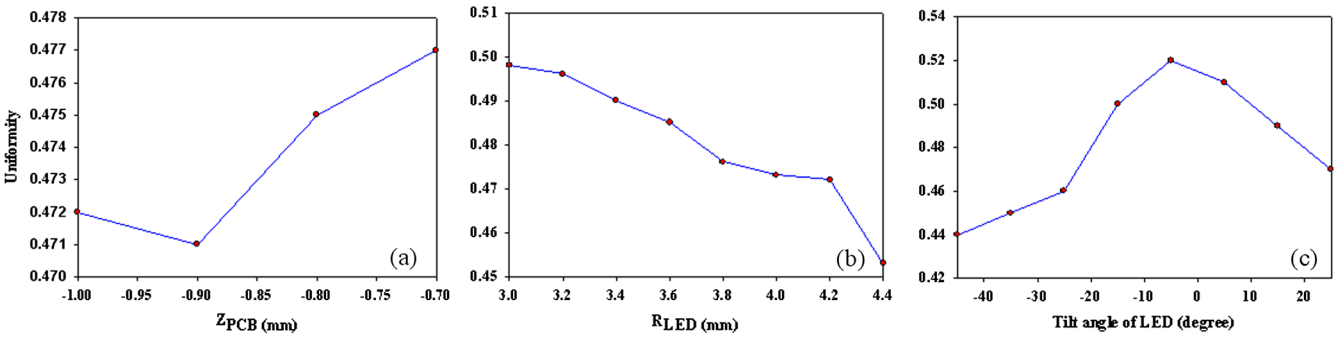

Fig. 16 Simulation results for uniformity of light with (a) moving the PCB on the Z axis, (b) moving the LED on the radial direction, and (c) tilting the LED surface.

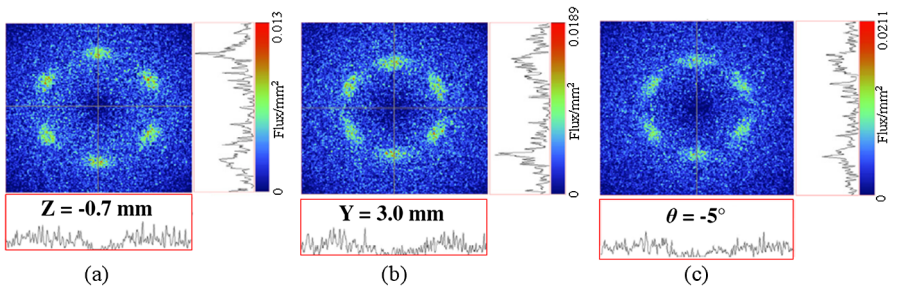

Fig. 17 Power distribution on the image plane with the three best uniformity cases: (a) Z_{PCB} position is −0.7 mm, (b) R_{LED} position is 3 mm, and (c) tilt angle is −5 deg.

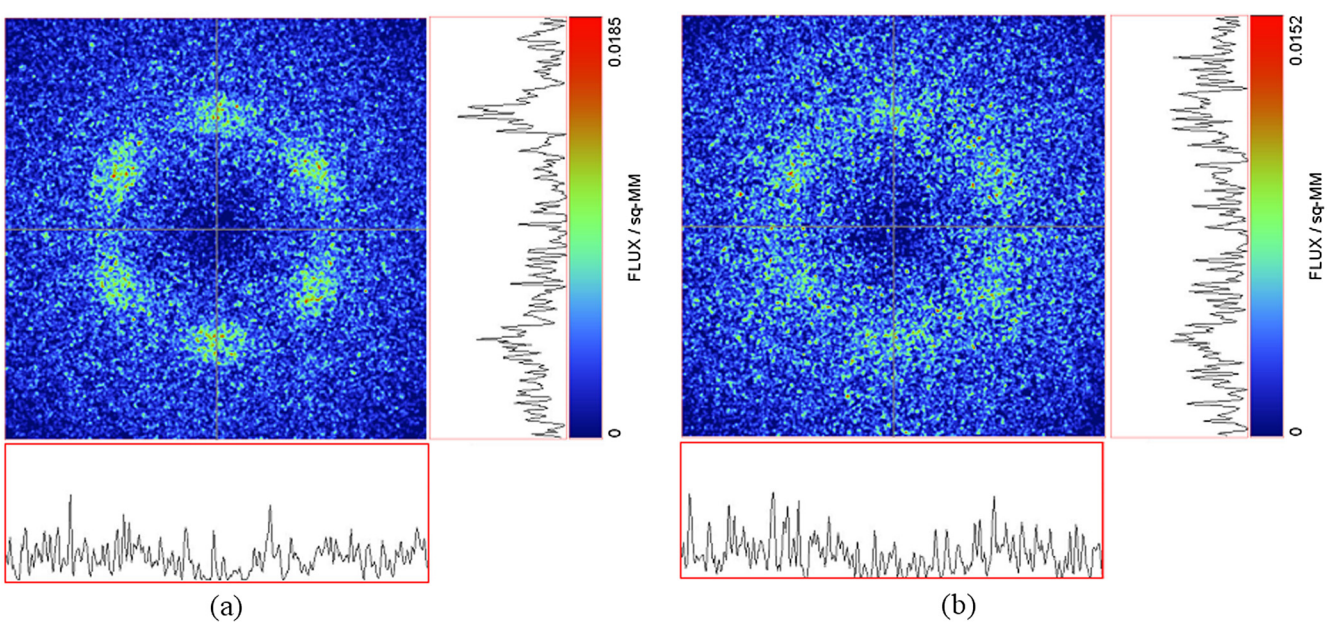

Fig. 18 Power distribution on the image plane when the TVW is included (a) without coating and (b) with a single-layer coating.

Figure 21(a) shows an ellipse with semi-major axis a (equals inner radius of the capsule shell), semi-minor axis b, and distance from the center to focal point c. The relation among these dimensions can be written as Eqs. (5) and (6), where R is the curvature of the ellipse. Since the size of a is 5 mm and b is 3.34 mm, c can be determined by Eq. (4) which is 3.72 mm. Hence, the LEDs are placed at the focal points during simulation. The simulation result is shown in Fig. 21(b), where the six light spots problem can be solved by placing the LEDs on the focal plane. However, the light intensity is very high at the center region, which causes the illumination uniformity decrease, and the LED cannot be treated as a point light source, as it still has the stray light problem. Therefore, the uniformity is only 0.6; this is lower than the optimized RICE system in which the light uniformity is 0.69. It means this paper proposes an

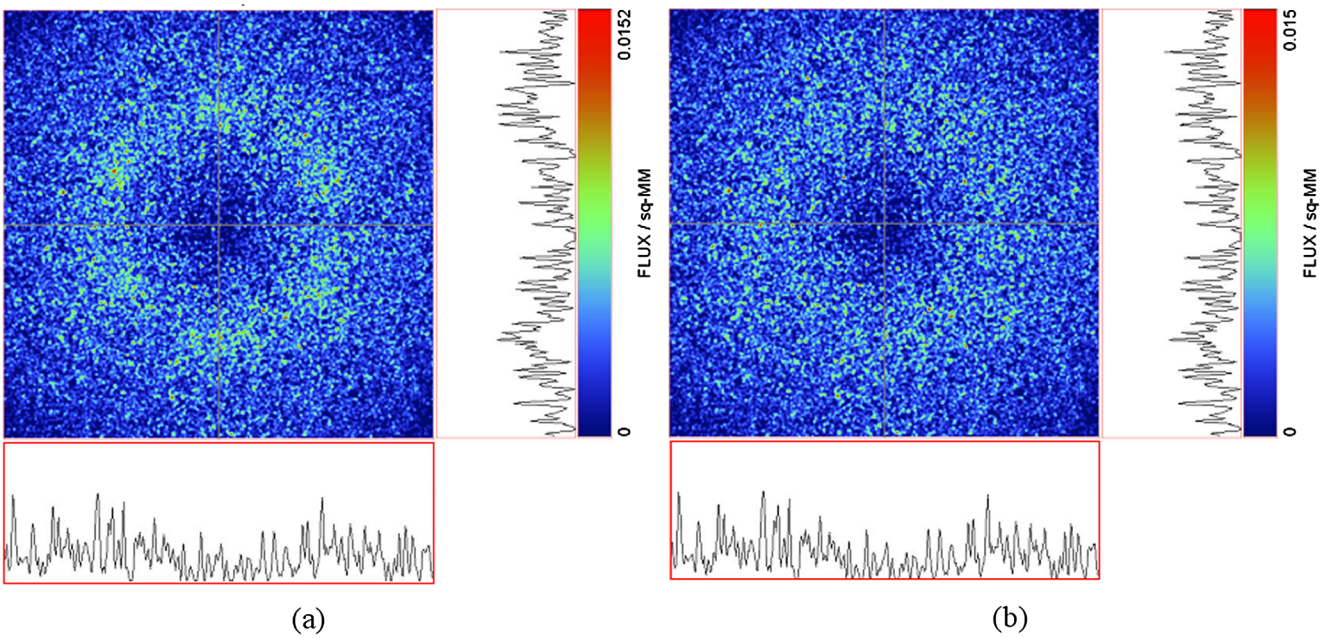

Fig. 19 Power distribution on the image plane when the TVW is coated on both sides with (a) single-layer and (b) multilayer coating.

Table 2 The simulation results of various coating method on the TVW.

		Coating type (inner/outer)				
Optical property		Non/Non	Single layer/Non	Multilayer/Non	Single layer/Single layer	Multilayer/Multilayer
TVW reflectance	Inner	0.053	0.0075	Close to 0	0.0075	Close to 0
	Outer	0.053	0.053	0.053	0.0075	Close to 0
Uniformity		0.52	0.57	0.61	0.63	0.69

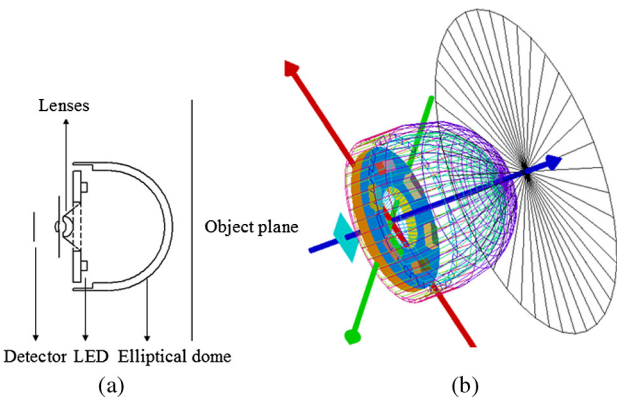

Fig. 20 The (a) structure and (b) simulation model of FICE system.

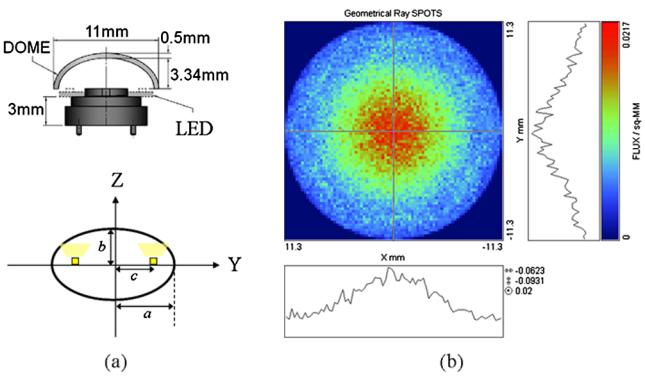

Fig. 21 (a) In the FICE system, the LEDs are placed at the focal plane. (b) Power distribution of FICE system shows that the six light spots disappear by placing the LEDs on the focal plane.

optimal design of the illumination system in RICE, and the uniformity is better than the FICE system.

$$a^2 = b^2 + c^2 \tag{5}$$

$$R = -\frac{a^2}{b} \tag{6}$$

4.4 *Analysis of the Temperature Effect of LED in RICE System*

Typically, the temperature can affect the performance of LEDs, for example, by decreasing the internal quantum efficiency, external efficiency, and maximum output power; shortening the device lifetime; and shifting the emission peak of wavelength when temperature increases.[16] In this

paper, the most important issue is the shift of the peak emission wavelength with the temperature, because when the peak of spectrum shifts to another wavelength, it can affect the color rendering index (CRI) of the light source. For biomedical image applications, the image cannot have a color difference.

Usually, the heat is caused by the nonradiative recombination, which is because the electron energy is converted to vibrational energy of lattice atoms (phonons). When the temperature increases, the electrons will escape from the quantum well, decreasing the energy band gap of semiconductors. Therefore, the peak emission wavelength increases. This issue can be expressed by the Varshni formula as shown in Eq. (7), where α and β are fitting parameters.[17]

$$E_g = E_g|_{T=\mathrm{OK}} - \frac{\alpha T^2}{T+\beta} \tag{7}$$

Hence, an experiment is carried out to measure the shift of emission peak. The procedure is begun by placing the LED inside an integrating sphere. A power supply is used to supply the LED DC current which is 10 mA, and the environment temperature is about 25°C. The diagnosis duration often takes 8 h using a capsule endoscope, so this experiment measured the spectrum at the beginning and after driving the LED for 8 h. Finally, the initial spectrum of the LED is compared to the spectrum after driving the LED for 8 h, and the experimental results are shown in Fig. 22. It reveals that the peak of wavelength does not change after driving the LED for 8 h, the peaks of the spectra are 477 and 478 nm. However, the output power is decreased due to the temperature effect, which does affect the CRI of the light source, and the color difference is computed by the formula of CIELAB color space, where ΔE^* is 4.78. However, this can be solved by color calibration, the method is using color mapping to reconstruct the real color.[18]

4.5 *Stray Radiation Analysis in RICE*

In order to verify the accuracy of the stray radiation in this system, the sampling concept should be considered. In general, the stray radiation causes nonuniformity in an optical

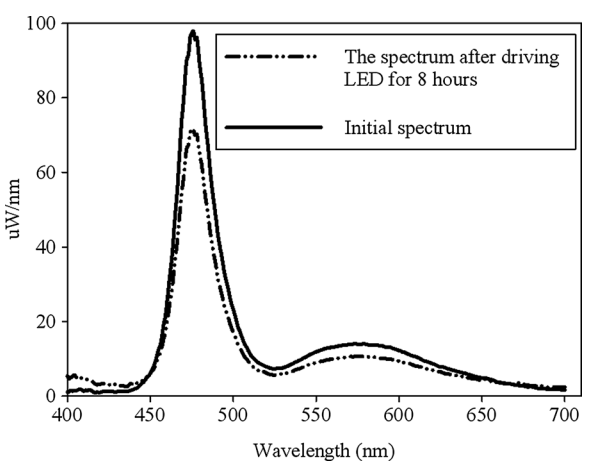

Fig. 22 Comparison of the initial spectrum (solid line) to another spectrum after driving the LED for 8 h (dashed-dot line). It reveals that the peak wavelength did not change after driving the LED for 8 h, but the power intensity decreased due to the temperature effect.

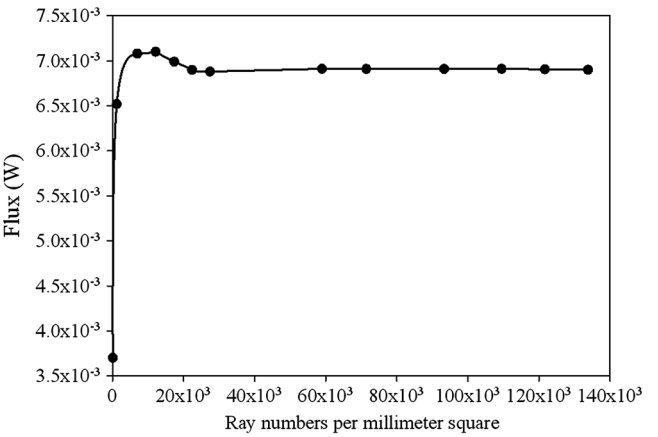

Fig. 23 Simulation results between ray number density and stray radiation level. The curve approaches a static state when the ray number density is higher than 30×10^3 rays/mm^3.

system, so this result will vary with the given number of sampling. Thus, the principle of weight-equivalent sampling, or the uniformity principle of ray number density, is adopted to evaluate the stray light level.[19,20] In this case, the ray number was changed to simulate the stray radiation level in different ray number densities, where the ray number density is defined as a ray sample number per unit area. Figure 23 shows the relation between ray number density and stray radiation level, the curve approaches a static state when the ray number density is higher than 30×10^3 rays/mm^2. In this work, the ray number density is 121655 in all the simulation results to meet a high accuracy model.

5 Conclusions and Discussions

This work focuses on illumination design. First, a model radial imaging capsule endoscope was constructed. It comprises doublet lenses, a cone mirror, a transparent view window, a tube-shaped object, a lighting source, and an image plane. Second, the specifications of all of the elements in the model were set and the model was used in a simulation. An experiment was also carried out to establish the accuracy of the model, which was constructed in software. Third, various simulations were run using different methods to design an optimal system. These methods involved changing the PCB and the LED position, tilting the LED, coating the TVW, and even cutting out the front of the cone mirror to reduce the intensity of the direct stray light. Finally, the simulation of the optimal design yielded a light uniformity close to 0.7. Table 3 compares such an optimal design with a previous design.[6] Cutting the cone mirror clearly reduces the direct stray light and increases the uniformity by more than 115% for all methods. Another important issue is that this paper proposes an optimal design of the illumination system in RICE, and the uniformity is better than the FICE system.

Since the LED is highly directive, light propagation concentrates in the front region, causing nonuniformity. A diffuser sheet can be placed on the LED surface to reduce the high directionality. When the light is emitted from the surface of the LED, it firstly scatters in the diffuser sheet, changing the direction of propagation of the rays and increasing the uniformity of the lighting of the space in the capsule endoscope. Therefore, the goal of our future work will be

Table 3 The comparison of illumination design between optimum and previous design.

Methods	Uniformity		Increase percentage (Previous design/ Optimum design)
	Previous design (without cut cone mirror)	Optimum design (cut cone mirror)	
Cutting cone mirror	NA	0.5	NA
Moving PCB	0.41	0.48	117%
Moving LED	0.43	0.50	116%
Tilt LED angle	0.45	0.52	116%
Multilayer coating	0.60	0.69	115%

to design a diffuser sheet to provide uniformity of lighting in a RICE system.

Acknowledgments

This paper was particularly supported by the Aim for the Top University Plan of the National Chiao Tung University, the Ministry of Education of Taiwan, the National Science Council of Taiwan (Contract No. NSC 101-2220-E-009-032, 101-2218-E-039-001, NSC 101-2623-E-009-006-D), and Delta Electronics Incorporation (Contract No. NCU-DEL-101-A-04). Han-Min Feng and Ted Knoy are appreciated for their editorial assistance. The authors also want to thank them for providing experimental assistance and related information.

References

1. H. H. Hopkins and N. S. Kapany, "A flexible fiberscope, using static scanning," *Nature* **173**(4392), 39–41 (1954).
2. G. Iddan et al., "Wireless capsule endoscopy," *Nature* **405**(6785), 417–418 (2000).
3. M. Ou-Yang and W. D. Jeng, "Design and analysis of radial imaging capsule endoscope (RICE) system," *Opt. Express* **19**(5), 4369–4383 (2011).
4. M. Ou-Yang et al., "Optimizing the depth of field for short object distance of capsule endoscope," *Proc. SPIE* **6859**, 68591Q (2008).
5. V. N. Mahajan, "Optical imaging and aberrations, part I: ray geometrical optics," Chapter 1 in *Gaussian Optics*, p. 7, SPIE Press, Bellingham, Washington (1998).
6. W. D. Jeng et al., "Design of illumination system in ring field capsule endoscope," *Proc. SPIE* **7893**, 78930E (2011).
7. A. Desrosières, *The Politics of Large Numbers: A History of Statistical Reasoning*, pp. 147–177, Harvard University Press, Cambridge, Massachusetts (1998).
8. Y. Dodge, *The Oxford Dictionary of Statistical Terms*, 6th ed., pp. 78–99, Oxford University Press, Wellington Square, Oxford, United Kingdom (2003).
9. Wikipedia, "Standard deviation," http://en.wikipedia.org/wiki/Standard_deviation/ (1 Feburary 2011).
10. C. C. Sun et al., "Precise optical modeling for LED lighting verified by cross correlation in the midfield region," *Opt. Lett.* **31**(14), 2193–2195 (2006).
11. C. C. Sun et al., "Precise optical modeling for LED lighting based on cross-correlation in mid-field region," *Opt. Lett.* **31**(14), 2193–2195 (2006).
12. W. T. Chien, C. C. Sun, and I. Moreno, "Precise optical model of multi-chip white LEDs," *Opt. Express* **15**(12), 7572–7577 (2007).
13. M. Born and E. Wolf, *Principles of Optics: Electromagnetic Theory of Propagation, Interference and Diffraction of Light*, 7th ed., p. 952, Cambridge University Press, Cambridge (1999).
14. W. J. Smith, *Modern Optical Engineering: The Design of Optical Systems*, 3rd ed., pp. 615–617, McGraw-Hill, New York (2000).
15. M. Ou-Yang et al., "Image stitching and reconstructing image of intestines captured using radial imaging capsule endoscope (RICE)," *Opt. Eng.* **51**(5), 057004 (2012).
16. Y. G. Xi et al., "Junction temperature in ultraviolet light-emitting diodes," *Japan. J. Appl. Phys.* **44**(10), 7260–7266 (2005).
17. Y. Xi et al., "Junction and carrier temperature measurements in deep-ultraviolet light-emitting diodes using three different methods," *Appl. Phys. Lett.* **86**(3), 031907 (2005).
18. T. Johnson, "Methods for characterizing colour scanners and digital cameras," *Displays* **16**(4), 183–191 (1996).
19. X. L. Xia, Y. Shuai, and H. P. Tan, "Calculation techniques with the Monte Carlo method in stray radiation evaluation," *J. Quant. Spectr. Rad. Trans.* **95**(1), 101–111 (2005).
20. H. P. Tan et al., "Reliability of stray light calculation code using the Monte Carlo method," *Opt. Eng.* **44**(2), 023001 (2005).

Mang Ou-Yang received a BS degree in control engineering in 1991 and MS and PhD degrees in electro-optical engineering in 1993 and 1998 from National Chiao-Tung University, Hsinchu, Taiwan. He worked for the Precision Instrument Development Center, National Science Council of Taiwan and was in charge of optical metrology for space applications from 1994 to 2000. Thereafter, he worked for Klaser Technology Co. as the leader of the R&D group for developing projection display technology. Since 2004, he has been at the Institute of Optical Sciences, National Central University, Jhongli, Taiwan, as an assistant professor. Since 2009, he has been at the Department of Electrical and Computer Engineering, National Chiao-Tung University, Taiwan, as a professor. His research interests are related to optoelectronics industrial instrumentation development, including biomedical optics, microthermal sensors, readout electronics, and projection display technology.

Wei-De Jeng received his BS degree from the Department of Electrical Engineering, National Taiwan Ocean University, Taiwan, in 2008 and his MS degree from the Department of Optics and Photonics Engineering, National Central University, Taiwan, in 2010. He is currently studying toward the PhD degree at the National Chiao-Tung University. His research interest focuses on the biomedical field.